# Biochemical and Spectroscopic Characterization of the Covalent Binding of Heme to Cytochrome b 6 †

**ARTICLE** *in* BIOCHEMISTRY · MAY 2004

Impact Factor: 3.02 · DOI: 10.1021/bi036093p · Source: PubMed



**5 AUTHORS**, INCLUDING:

Catherine de Vitry
French National Centre for Scientific Research
**31** PUBLICATIONS **1,016** CITATIONS
SEE PROFILE

Alain Desbois
Atomic Energy and Alternative Energies Com…
**48** PUBLICATIONS **972** CITATIONS
SEE PROFILE

Francesca Zito
French National Centre for Scientific Research
**31** PUBLICATIONS **997** CITATIONS
SEE PROFILE

# Biochemical and Spectroscopic Characterization of the Covalent Binding of Heme to Cytochrome $b_6$[†]

Catherine de Vitry,*[,‡] Alain Desbois,[§] Virginie Redeker,[||,⊥] Francesca Zito,[‡,#] and Francis-André Wollman[‡]

*Physiologie Membranaire et Moléculaire du Chloroplaste CNRS UPR 1261, Institut de Biologie Physico-Chimique CNRS FRC 550, 13 Rue Pierre et Marie Curie, 75005 Paris, France, Département de Biologie Joliot-Curie, CEA and CNRS URA 2096, Service de Biophysique des Fonctions Membranaires, CEA/Saclay, F-91191 Gif-sur-Yvette Cedex, France, and Ecole Supérieure de Physique et de Chimie Industrielles de la Ville de Paris, Neurobiologie et Diversité Cellulaire, CNRS UMR 7637, 10 Rue Vauquelin, 75005 Paris, France*

*Received November 21, 2003; Revised Manuscript Received February 4, 2004*

ABSTRACT: The three-dimensional structure of the cytochrome $b_6f$ complex disclosed the unexpected presence of a new heme $c_i$ [Stroebel, D., Choquet, Y., Popot, J.-L., and Picot, D. (2003) *Nature 426*, 413−418; Kurisu, G., Zhang, H., Smith, J. L., and Cramer, W. A. (2003) *Science 302*, 1009−1014]. Here we present a biochemical, spectroscopic, and mutagenesis study of this unusual heme binding in *Chlamydomonas reinhardtii*. As predicted by the structure data, we identify a $Cys^{35}$-containing proteolytic fragment ($Tyr^{25}$−$Lys^{111}$) from cytochrome $b_6$ as a peptide that covalently binds a heme. Resonance Raman spectra of cyt $b_6f$ complexes show particular frequencies in $\nu_2$, $\nu_3$, $\nu_4$, and $\nu_8$ regions that identify this extra heme as a ferrous *c*′-like heme under a five-coordinated high-spin state. The set of frequencies is consistent with a coordination by either a water molecule or a hydroxide ion. Other changes in resonance Raman bands, observed in the mid- and low-frequency regions, point to a modification in conformation and/or environment of at least one *b* heme methyl and/or propionate group. Site-directed mutagenesis of apocytochrome $b_6$, leading to a $Cys^{35}$Val substitution, generates *Chlamydomonas* strains that are unable to assemble cytochrome $b_6f$ complexes. On the basis of the mutant phenotype, we discuss the participation, in the covalent binding of heme $c_i$, of the nuclear CCB factors that we identified previously as controlling the apo to holo conversion of cytochrome $b_6$ [Kuras, R., de Vitry, C., Choquet, Y., Girard-Bascou, J., Culler, D., Büschlen, S., Merchant, S., and Wollman, F.-A. (1997) *J. Biol. Chem. 272*, 32427−32435].

Cytochrome (cyt)[1] *bc* complexes are ubiquitous in electron transfer chains. They catalyze electron transfer from a liposoluble carrier to a water soluble protein and contribute to the formation of a transmembrane proton gradient. In higher plants and algae, chloroplasts, and cyanobacteria, cyt $b_6f$ catalyzes electron transfer from plastoquinol to plastocyanin or cyt $c_6$ and contains eight subunits: cyt *f*, cyt $b_6$, subunit IV, Rieske protein, and four small subunits (PetG, PetL, PetM, and PetN) comprising a single transmembrane α-helix (reviewed in refs *1*−*4*). Four redox cofactors have been identified for a long time in the cyt $b_6f$ complex: one *c*-type heme covalently attached by two thioether bonds to two cysteines of cyt *f*, two *b*-type hemes in cyt $b_6$ (i.e., a low-potential heme $b_l$ and a high-potential heme $b_h$), and an $Fe_2S_2$ cluster in the Rieske iron−sulfur protein. A chlorophyll *a* (chl *a*) and a carotenoid are also present in cyt $b_6f$ complexes (reviewed in ref *5*). Mitochondrial cyt $bc_1$ (*6*−*8*) and chloroplast cyt $b_6f$ complexes (*9*, *10*) crystallize in a dimeric form and exhibit overall similar organizations. In particular, their *b*-type hemes present similar arrangements (*11*−*13*), but there are differences in heme peroxidase activity when these cytochromes are placed under denaturing conditions. Whereas no such activity is detected with the *b* cytochromes from mitochondrial and most bacterial $bc_1$ complexes after they are boiled in the presence of SDS, cyt $b_6$ still exhibits peroxidase activity (reviewed in ref *14*). We tested various denaturing conditions, including acetone acid treatment, i.e., conditions expected to destroy interactions

[†] This work was supported by the Centre National de la Recherche Scientifique.

* To whom correspondence should be addressed. E-mail: catherine.devitry@ibpc.fr. Fax: 33 1 58 41 50 22. Phone: 33 1 58 41 50 55.
[‡] Institut de Biologie Physico-Chimique CNRS FRC 550.
[§] CEA/Saclay.
[||] CNRS UMR 7637.
[⊥] Present address: Laboratoire d'Enzymologie et de Biochimie Structurales, CNRS UPR 9063, avenue de la terrasse, 91190 Gif-sur-Yvette, France.
[#] Present address: Physico-Chimie Moléculaire des Membranes Biologiques, CNRS and Université Paris-7 UMR 7099, Institut de Biologie Physico-Chimique, CNRS IFR 550, 13 rue Pierre et Marie Curie, 75005 Paris, France.

[1] Abbreviations: chl, chlorophyll; Cm, meso carbon; Cter, C-terminal; cyt, cytochrome; HG, Hecameg [6-*O*-(*N*-heptylcarbamoyl)-methyl-α-D-glycopyranoside]; MALDI-TOF, matrix-assisted laser desorption ionization time-of-flight; *m*/*z*, mass-to-charge ratio; Nter, N-terminal; PAGE, polyacrylamide gel electrophoresis; Pr, propionate; SDS, sodium dodecyl sulfate; TMBZ, 3,3′,5,5′-tetramethylbenzidine; RR, resonance Raman; Tricine, *N*-[2-hydroxy-1,1-bis(hydroxymethyl)-ethyl]glycine [*N*-tris(hydroxymethyl)methylglycine].

10.1021/bi036093p CCC: $27.50 
Published on Web 03/09/2004

between the *b* hemes and their apoproteins, and concluded with an unusual tight binding of one heme to cyt $b_6$ (*14*). Mass spectrometry applied to purified cyt $b_6f$ complexes of *Chlamydomonas reinhardtii* (this work) as well as to cyt complexes of spinach and cyanobacterium *Mastigocladus laminosus* (*15*) confirmed a tight binding of heme to cyt $b_6$.

Three-dimensional crystals of cyt $b_6f$ complexes from *C. reinhardtii* (*16*) and *M. laminosus* (*17*) have recently been analyzed at 3.0−3.1 Å resolution. The *Chlamydomonas* structure, disclosed a new type of heme, and Stroebel *et al*. (*16*) named $c_i$, bound to $Cys^{35}$ of cyt $b_6$ and was liganded via a water molecule or a hydroxide ion to a propionate group of heme $b_h$. The presence of an extra heme in cyt $b_6$ was confirmed upon refinement of the analysis of the *Mastigocladus* crystal (*17*).

Surprisingly, this heme had not been spectroscopically detected in purified $b_6f$ complexes except in pyridine hemochrome spectra. Pyridine hemochrome difference spectra of the purified cyt $b_6f$ complex reveal an extra heme whose spectrum is red-shifted compared to that of cyt *f* (*16*, *17*), as in the case of trypanosome heme $c_1$ which is bound to the apoprotein through only one thioether bond (*18*). *In vivo*, a cytochrome named "cyt *G*" has been identified by optical spectroscopy as a high-spin (HS) cyt *c*′ that interacts with heme $b_h$ (*19*, *20*). However, the possible correspondence between cyt *G* and heme $c_i$ remains to be established. Apart from the crystal structure, little is known about heme $c_i$. Therefore, studies of the biochemical, spectroscopic, and biogenesis properties of this atypical heme are timely.

In this work, we characterized the heme covalently bound to cyt $b_6$ in *C. reinhardtii*, using proteolysis treatments, mass spectrometry, resonance Raman (RR) spectroscopy of the purified $b_6f$ complex, and site-directed mutagenesis of the chloroplast *petB* gene encoding cyt $b_6$. We identified covalent heme binding within the $Tyr^{25}$−$Lys^{111}$ peptide of cyt $b_6$. RR data detect free vinyls for the *b* hemes of cyt $b_6$, but suggest an interaction of one of their propionate and/or methyl group(s) with heme $c_i$. We also provide an RR spectroscopic characterization of heme $c_i$ as a ferrous *c*′-type heme in a five-coordinate (5c) HS state. Substitution of $Cys^{35}$, which is involved in the unique thioether binding of heme $c_i$, shows an immunodetected cyt $b_6$ doublet characteristic of *ccb* mutants, which probably define the biogenesis pathway for heme $c_i$.

## EXPERIMENTAL PROCEDURES

*Growth Conditions. C. reinhardtii* strains were grown in Tris-acetate-phosphate (TAP, pH 7.2) at 25 °C under 6 $\mu$E $m^{-2}$ $s^{-1}$ continuous illumination and collected during the exponential phase of growth at a density of $2 \times 10^6$ cells/mL.

*Purification of Thylakoid Proteins.* Thylakoid membranes were purified and resuspended in 10 mM Tricine-NaOH (pH 8.0) containing protease inhibitors (200 $\mu$M phenylmethanesulfonyl fluoride, 1 mM benzamidine, and 5 mM $\epsilon$-aminocaproic acid) as described in ref *21*. Cyt $b_6f$ dimer complexes were extracted with a 25 mM Hecameg (HG) solubilization of thylakoid membranes as previously described (*22*). To separate the Rieske protein and some small subunits from the rest of the complex, cyt $b_6f$ complexes were monomerized as follows, after 10 to 30% (w/w) sucrose gradient centrifugation. HG was added up to 70 mM to the original buffer [20 mM Tricine-NaOH (pH 8.0), 3 mM $MgCl_2$, 3 mM KCl, 20 mM HG, and 0.1 g/L egg phosphatidylcholine], and the protein complex was incubated on ice for 30 min. The monomer preparation was then adsorbed onto a hydroxylapatite column equilibrated with 20 mM Tricine-NaOH buffer (pH 8.0) containing 30 mM HG; many proteins, including the Rieske protein and some small subunits, eluted with 150 mM ammonium phosphate (pH 8.0) containing 30 mM HG. The monomerized cyt $b_6f$ complex was eluted with 400 mM ammonium phosphate (pH 8.0) containing 30 mM HG. To separate the monomer from the dimer and from free pigments, the monomerized cyt $b_6f$ complex was layered onto a 10 to 30% (w/w) sucrose gradient in 20 mM Tricine-NaOH (pH 8.0), 20 mM HG, 0.1 g/L egg phosphatidylcholine buffer and centrifuged at 35 000 rpm (200000*g*) for 15 h in the SW41 Ti rotor of an L8 ultracentrifuge (Beckman). The brown band of the cyt $b_6f$ monomer was collected with a syringe (*23*). The cyt $b_6f$ monomer was concentrated by adsorption onto a hydroxylapatite column equilibrated with 20 mM Tricine-NaOH buffer (pH 8.0) containing 30 mM HG and eluted with 400 mM ammonium phosphate (pH 8.0) containing 30 mM HG. For trypsin digestion, the cyt $b_6f$ monomer was dialyzed in 20 mM Tricine (pH 8.0) and 20 mM HG. Absorption spectra were recorded on a Hewlett-Packard HP 8453 spectrophotometer. Extinction coefficients for cyt *f* ($\epsilon_{554} = 26\,000$ $M^{-1}$ $cm^{-1}$) and for chl *a* ($\epsilon_{667} = 75\,000$ $M^{-1}$ $cm^{-1}$) were used (*5*). The cyt $b_6f$ complex concentration was expressed in terms of heme *f* concentration.

*Protein Analysis and Peroxidase Activity Staining.* Polypeptides were separated on 12 to 18% SDS−polyacrylamide gels containing 8 M urea and stained using either Coomassie Brilliant Blue or silver nitrate (*21*). Proteins were electrotransferred onto Immobilon NC membranes in a semidry blotting system at 0.8 mA $cm^{-2}$ for ∼30 min. Antisera raised against peptides of the N-terminus ($S^2$KVYDWFEERLEIQ$^{15}$) and the C-terminus ($L^{204}$MIRKQGISGPL$^{215}$) of cyt $b_6$ or against cyt *f* were used at a 1/200 dilution and detected using $^{125}$I-labeled protein A. Heme staining was detected by peroxidase activity of the heme binding subunits either on gels using 3,3′,5,5′-tetramethylbenzidine (TMBZ) (*24*) or on blots using the very sensitive chemiluminescence peroxidase method Super Signal West Femto Maximum Sensitivity Substrate (Pierce). Detection of heme staining on blots is derived from Western blotting but uses neither primary antibody nor secondary antibody−peroxidase enzyme conjugate. The blot was washed just after transfer in phosphate-buffered saline for 1 min, pressed in filter paper to remove the excess buffer, incubated in Super Signal Substrate luminol and enhancers for 5 min, and briefly pressed in filter paper. Light emission resulting from peroxidase activity on the luminol substrate was detected using high-performance chemiluminescence films (Hyperfilm ECL, Amersham Pharmacia).

*Lys-C Proteolysis for Peroxidase Activity Staining.* One hundred microliters of a 20 $\mu$M cyt $b_6f$ complex preparation deprived of Rieske protein was separated in its constitutive subunits on a low-acrylamide concentration gel (12% SDS−PAGE) to favor subsequent access to proteases and peptide release. Side lanes from the gels were TMBZ-stained to

localize cyt $b_6$. The band containing cyt $b_6$ was cut out and crushed in a 1 mL syringe through a very fine grid. One hundred milligrams of crushed gel was mixed with 50 $\mu$L of water in the presence or absence of 5 $\mu$g of endoproteinase Lys-C for 15 min (sequencing-grade, Roche); the gel was then incubated at 37 °C for 6 h under vigorous shaking with 200 $\mu$L of 25 mM Tris buffer (pH 8.5) containing 1 mM EDTA and 0.1% SDS. Crushed gel samples were incubated in loading buffer for 30 min before polypeptides were separated on a second 12 to 18% SDS−polyacrylamide gel containing 8 M urea, blotted, and either stained with heme with the very sensitive chemiluminescence peroxidase method Super Signal West Femto Maximum Sensitivity Substrate (Pierce) or reacted with specific antibodies.

*Mutagenesis and Plasmids*. Plasmid pdWB (*25*) which encompasses the whole *petB*-coding region was used to perform site-directed mutagenesis according to the method of Kunkel (*26*). The PdWB single strand was used for annealing with the following mutagenic oligonucleotide (B35V, AAAGTAATACCACCAAT**TAC**GTAGAAAA-TATTTACG). Bold letters indicate the mutated nucleotides, while the new restriction site (*Sma*BI) generated by a silent mutation is underlined. This leads to plasmid pb35V. Plasmid pbK35V was constructed by introducing the 1.9 kb *Sma*I−*Eco*RV fragment of plasmid pUC-atpX-AAD containing the *aadA* cassette (*27*), in the same orientation as the *petB* gene in the *Nsi*I site of plasmid pb35V. Wild-type and Δ*petB* strains (*25*) were transformed by tungsten particle bombardment (*28*) using a device, operating under vacuum, built in the laboratory (*29*). Phototrophic transformants were selected on a minimum medium at 60 $\mu$E m$^{-2}$ s$^{-1}$. Transformants containing the *aadA* cassette were selected for growth on TAP−spectinomycin medium as previously described (*25*).

*Mass Spectrometry*. Molecular masses of the different subunits of $b_6f$ complexes were determined by matrix-assisted laser desorption ionization time-of-flight mass spectrometry (MALDI-TOF MS) using a MALDI-TOF mass spectrometer Voyager-Elite biospectrometry workstation (Perseptive Biosystems, Framingham, MA) equipped with a nitrogen laser (237 nm). When we used a 4 $\mu$M solution of the $b_6f$ complex in 400 mM ammonium phosphate (pH 8.0) containing 30 mM HG and protease inhibitors (200 $\mu$M phenylmethanesulfonyl fluoride, 1 mM benzamidine, and 5 mM $\epsilon$-aminocaproic acid), the sample was diluted 5-fold in a solution of 5% aqueous trifluoroacetic acid and then mixed volume to volume with a matrix of sinapinic acid (saturated solution in 30% acetonitrile and 0.1% aqueous trifluoroacetic acid). When we used a 6 $\mu$M solution of the $b_6f$ complex without Rieske in solution in 400 mM ammonium phosphate (pH 8.0), 30 mM HG, and protease inhibitors (200 $\mu$M phenylmethanesulfonyl fluoride, 1 mM benzamidine, and 5 mM $\epsilon$-aminocaproic acid), the sample was first diluted 2-fold in a solution of 1% aqueous trifluoroacetic acid and then mixed with 1 volume of a matrix of sinapinic acid. Spectra were acquired in the positive and linear mode (accelerating voltage of 25 kV, grid voltage of 90%, guide wire of 0.3%, and 275 ns delayed extraction). The calibration was performed using apomyoglobin doubly charged monomer (*m*/*z* 8476.78), the singly charged monomer (*m*/*z* 16 952.56), and the dimer (*m*/*z* 33 904).

After enzymatic cleavage, the proteolytic peptide solution was diluted to ∼1−3 pmol/L in a trifluoroacetic acid solution to reach a final trifluoroacetic acid concentration of 1%. After cocrystallization with a matrix of 2,5-dihydroxybenzoic acid (saturated solution in 0.1% aqueous trifluoroacetic acid) and sinapinic acid (saturated solution in 30% acetonitrile and 0.1% aqueous trifluoroacetic acid), samples were analyzed by MALDI-TOF MS using a Voyager-STR system (Perseptive Biosystems, Framingham, MA) in the positive and both linear (accelerating voltage of 20 kV, grid voltage of 95%, and 400 ns delayed extraction) and reflectron mode (accelerating voltage of 20 kV, grid voltage of 73%, and 210 ns delayed extraction). Peptides released from the different protein subunits upon Lys-C digestion were identified by comparing experimental masses with theoretical masses of the nonmodified peptides.

*Lys-C Digestion for Mass Spectrometry Analysis.* The $b_6f$ complex used for Lys-C cleavage was a 6 $\mu$M solution in 400 mM ammonium phosphate (pH 8.0) containing 30 mM HG diluted twice in $H_2O$ for the digestion. Extensive Lys-C (sequencing-grade, Roche) proteolysis of the $b_6f$ complex was performed overnight at 37 °C in 200 mM ammonium phosphate (pH 8.0) containing 15 mM HG and Lys-C [1/50 (w/w), enzyme/substrate ratio]. After digestion, samples were directly analyzed by MALDI-TOF mass spectrometry.

*Raman Spectroscopy*. The Raman spectra were recorded at 20 ± 1 °C using a Jobin-Yvon spectrometer (Ramanor HG2S-UV) with the 406.7 and 413.1 nm excitations of a $Kr^+$ laser (Coherent Innova) and the 441.6 nm excitation of a He/Cd laser (Liconix). Using laser radiant powers of 15−40 mW, the RR spectra (6−10 scans) were collected, imported, checked, and analyzed with Grams/32 (Galactic Industries). Under these conditions, the frequency precision is 0.5−1 cm$^{-1}$, depending on the signal-to-noise ratio (*11*, *13*).

## RESULTS

The $b_6$ hemes are noncovalently bound by a pair of histidine residues which serve as axial ligands to the iron atoms. The surprising persistence of a peroxidase activity for cyt $b_6$ under highly denaturing conditions (*14*) led us to investigate further the characteristics of this tight heme binding. Meanwhile, the resolution of the three-dimensional (3D) structure of cyt $b_6f$ complexes showed the presence of an additional *c*-type heme that should account for this property. Since cyt $b_6$ stains with TMBZ after SDS−PAGE, we tested whether we could localize further the protein domain implicated in this peroxidase activity. To this end, we prepared a pure cyt $b_6f$ complex monomer and separated cyt $b_6$ on a first SDS−PAGE dimension. We then treated cyt $b_6$ with an SDS-tolerant protease and separated its fragments on a second gel dimension. Using a sensitive chemiluminescent peroxidase activity test, we detected heme binding peptides and identified them with antibodies specific for the $Ser^2$−$Gln^{15}$ peptide at the $b_6$ N-terminus ($b_6$-Nter) and for the $Leu^{204}$−$Leu^{215}$ peptide at the $b_6$ C-terminus ($b_6$-Cter).

*Peroxidase Activity of Proteolytic Fragments after SDS−PAGE*. Two types of cyt $b_6f$ complexes were purified. The dimer contains one chl *a* and one carotene molecule (see the dotted line in Figure 1); the monomer has been treated

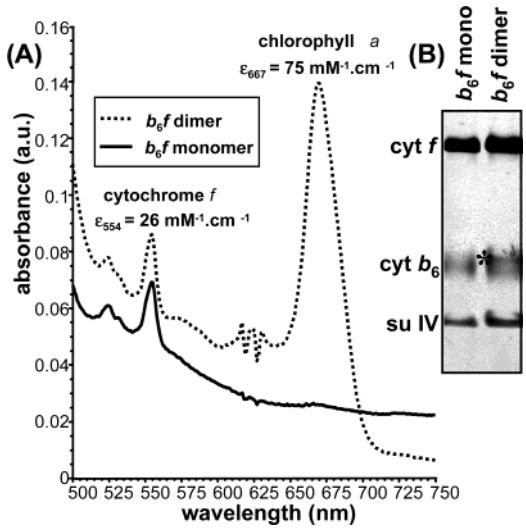


FIGURE 1: Characterization of purified $b_6f$ preparations. (A) Visible absorption spectra of purified, ascorbate-reduced, $b_6f$ preparations. (B) SDS−PAGE analysis of the $b_6f$ monomer without the Rieske protein ($b_6f$ mono) and the $b_6f$ dimer with the Rieske protein (denoted with an asterisk) after TMBZ peroxidase activity staining and silver protein staining.

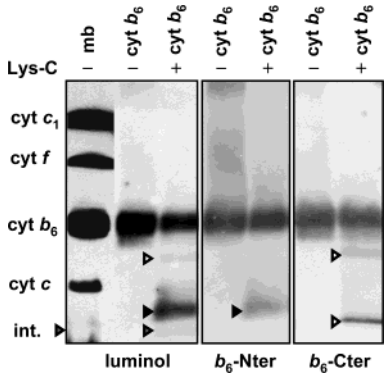


FIGURE 2: SDS−PAGE analysis of cyt $b_6$ proteolytic peptides. Membrane proteins (mb), purified cyt $b_6$ not treated (−) or treated (+) with protease Lys-C after luminol peroxidase activity staining (luminol) or immunodetection with antibodies against the N-terminus ($b_6$-Nter) or the C-terminus ($b_6$-Cter) of cyt $b_6$.

with 70 mM HG and purified on a hydroxylapatite column using buffers containing 30 mM HG and no lipid phosphatidylcholine. This treatment detaches most of chl *a*, the Rieske protein, and several small subunits (see the absence of chl *a* in the solid line in Figure 1A).

The polypeptide profile after SDS−PAGE of purified cyt $b_6f$ monomer and dimer complexes is shown in Figure 1B. Note the absence of the Rieske protein in the monomer preparation (the Rieske protein migrates just above cyt $b_6$ and is denoted with by an asterisk in the cyt $b_6f$ dimer lane in Figure 1B). In membrane preparations (Figure 2, left panel, lane 1), two mitochondrial cytochromes and two chloroplast cytochromes are heavily detected on blots by peroxidation of luminol. In order of decreasing apparent molecular mass, they correspond to chloroplast cyt *f*, mitochondrial cyt $c_1$, chloroplast cyt $b_6$, and mitochondrial cyt *c*. The cyt $b_6$ gel region was crushed and treated without (Figure 2, left panel, lane 2) or with (Figure 2, left panel, lane 3) protease Lys-C that has an endopeptidase activity on the carboxy-terminal end of Lys residues. Antibodies were then used to identify whether the fragments comprised the N-terminal (Nter) or C-terminal (Cter) domains. The major fragment displaying peroxidase activity is recognized by the $b_6$-Nter antibody (in Figure 2, see the black arrowheads in the left and middle panels). A large Cter fragment displaying peroxidase activity and a small Cter fragment not displaying peroxidase activity are recognized by the $b_6$-Cter antibody (in Figure 2, see the white arrowheads in the left and right panels). The smaller fragment displaying peroxidase activity is detected by peroxidation of luminol on blots (see the lower gray arrowhead in the left panel of Figure 2) but is recognized neither by the $b_6$-Nter nor by the $b_6$-Cter antibody. This fragment is therefore considered an internal one.

A schematic transmembrane structure of cyt $b_6$ of *Chlamydomonas* is presented in Figure 3. There are four transmembranes helices, one heme $b_l$ on the lumenal side and one heme $b_h$ on the stromal side of the membrane, and the two pairs of histidine axial ligands to the hemes being in helix B and helix D. The additional heme $c_i$ is represented with its $Cys^{35}$ covalent ligand and its axial ligand via a water molecule or a hydroxide ion to a propionate from heme $b_h$ (*16*). The protein sequence shows the potential sites of cleavage by protease Lys-C used for the experiment depicted in Figure 2, and the peptides used to raise $b_6$-Nter and $b_6$-Cter antibodies are indicated. The three peptides detected by peroxidation of luminol on blots are attributed for the larger to the $Tyr^{25}$−$Leu^{215}$ peptide, for the medium to the $Met^{1}$−$Lys^{111}$ peptide, and for the smaller to the $Tyr^{25}$−$Lys^{111}$ peptide. The $Tyr^{25}$−$Lys^{111}$ protein domain shaded dark gray in Figure 3, which comprises the first two transmembrane α-helices of cyt $b_6$, is the smaller internal Lys-C proteolytic fragment detected with luminol but not with the Nter and Cter antibodies. Its identification as a peroxidase activity-bearing fragment is therefore consistent with the binding of heme $c_i$ to $Cys^{35}$ in this polypeptide domain.

*Identification of Heme Binding by Mass Spectrometry.* The biochemical identification of the cyt $b_6$ protein domain implicated in covalent heme binding was performed by MALDI-TOF mass spectrometry that should allow us to observe some proteolytic peptides released from cyt $b_6f$ that would keep a bound heme.

First, we investigated by mass spectrometry a possible mass increment for apocyt $b_6$ that would be indicative of a tight heme binding. The mass spectra of the $b_6f$ complex isolated from *Chlamydomonas* with or without the Rieske protein reveal a molecular mass for cyt $b_6$ much higher than the theoretical molecular mass deduced from its polypeptide sequence (Figure 4). We compared masses of the largest subunits of cyt $b_6f$ complexes as measured by mass spectrometry with those calculated from their polypeptide sequences (Table 1). The mass increment of cyt $b_6$ (801 ± 24 Da) was consistent with the presence of a heme derivative or a regular *b* heme (616 Da) covalently bound to the protein, provided some unknown additional post-translational modifications occur.

We proteolyzed the $b_6f$ monomer complexes with the endoprotease Lys-C. The corresponding peptide pattern released by MALDI-TOF spectrometry is shown in Figure 5. We could attribute most of the peaks to cyt $b_6f$ peptides (Table 2). For instance, 86% of the cyt *f* polypeptide sequence could be unambiguously assigned to a specific set of peptides. Fifty percent of the cyt $b_6$ sequence could be unambiguously assigned to specific peptides, $Val^{4}$−$Lys^{24}$ and

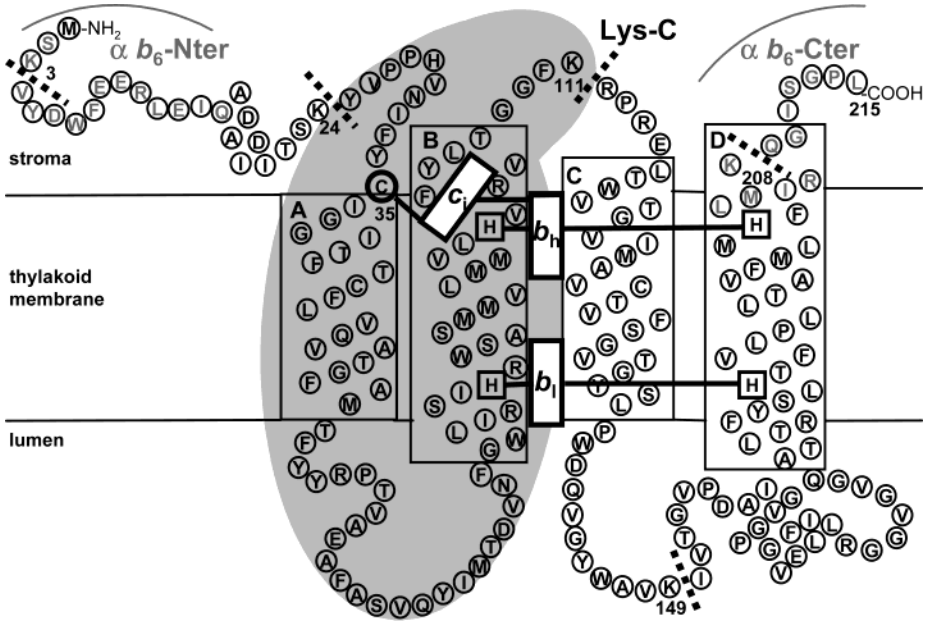


FIGURE 3: Schematic transmembrane structure of cyt $b_6$ of *C. reinhardtii*. Lys-C cleavage sites are indicated (small dashed lines). Peptides used to raise antibodies specific for the $b_6$ N-terminus ($Ser^2-Gln^{15}$, α $b_6$-Nter) and of the $b_6$ C-terminus ($Leu^{204}-Leu^{215}$, α $b_6$-Cter) are depicted in light gray. The smallest Lys-C proteolytic fragment ($Tyr^{25}-Lys^{111}$) detected with bound heme on a luminol blot and in mass spectrometry is colored dark gray. Heme $b_l$ and $b_h$ are depicted with their histidine axial ligands boxed. Heme $c_i$ is depicted with its $Cys^{35}$ covalent ligand circled in bold and numbered and its axial ligand via a water molecule or a hydroxide ion to a heme $b_h$ propionate.

Table 1: Average Protonated Masses Calculated from the Sequence (M calcd) and Measured by Mass Spectrometry (M measd) of the Large Subunits of $b_6f$ Complexes from *C. reinhardtii*

| protein | Nt[a] | AA[b] | *M* calcd (Da)[c] | *M* measd (Da) | Δ*m* (Da)[d] | covalent modifications |
|---|---|---|---|---|---|---|
| mature cyt *f* | d | 286 | 31249 | 31854 ± 36 | 605 ± 36 | addition of heme 616 |
| cyt $b_6$ | nd | 215 | 24165 | 24966 ± 24 | 801 ± 24 | Nter blocked, addition of heme |
| mature Rieske | d | 177 | 18404 | 18414 ± 22 | 10 ± 22 | |
| subunit IV | nd | 160 | 17442 | 17331 ± 17 | 111 ± 17 | Nter blocked, removal of $Met^1$ 131 |

[a] N-Termini (Nt) are determined (d) or blocked (nd); cyt $b_6$ and subunit IV have a blocked N-terminus (*21*). [b] The number of amino acid residues of the mature protein is given, including the Nter methionine in the case of cyt $b_6$ and subunit IV. [c] Masses of cyt $b_6$ and subunit IV are calculated with their first methionine. [d] Differences between calculated and measured masses (Δ*m*) confirm covalent binding of a heme to cyt *f* and suggest post-translational modification(s) of cyt $b_6$.

$Tyr^{25}-Lys^{111}$ (fifth and 35th entries in Table 2). The peptide map displayed a heme-bound cyt *f* $Tyr^1-Lys^{29}$ peptide (15th entry in Table 2) and a heme-bound cyt $b_6$ peptide carrying an oxidized methionine, $Tyr^{25}-Lys^{111}$ (35th entry in Table 2). This $Tyr^{25}-Lys^{111}$ cyt $b_6$ peptide corresponds to the Lys-C proteolytic fragment capable of peroxidation of luminol on blotting after SDS−PAGE.

*Resonance Raman Spectra.* Dimeric $b_6f$ complexes contain one chl *a* and one carotenoid per monomer. To remove the chl *a* contribution in the RR spectra, we succeeded in preparing a monomeric $b_6f$ complex depleted of chl *a* (see Experimental Procedures). Unfortunately, this preparation still retained the carotenoid molecule.

Because of different Soret band positions of the *b*- and *c*-type hemes of $bc_1-b_6f$ complexes, their respective contributions can be elucidated using different laser excitations: a 441.6 nm excitation enhances contribution from *b* hemes, whereas 406.7 and 413.1 nm excitations are better suited for *c* hemes (*11*, *13*). The RR spectra of dimeric cyt $b_6f$ from spinach (*13*) and monomeric cyt $b_6f$ from *Chlamydomonas* (Figure 6) exhibited similar individual contributions of hemes $b_h$, $b_l$, and *f* for the skeletal $\nu_2$ (1580 ± 1, 1585 ± 1, and 1590 ± 1 $cm^{-1}$), $\nu_4$ (1361 ± 1 $cm^{-1}$), and $\nu_8$ (347 ± 1, 350 ± 1, and 358 ± 1 $cm^{-1}$) modes. The spectra of monomeric cyt $b_6f$ from *Chlamydomonas* exhibited an improved signal-to-noise ratio due to the removal of the chl *a* molecule and the Rieske iron−sulfur protein. The better quality of the *Chlamydomonas* spectra allowed us to observe additional, although weak, contributions that we attribute to heme $c_i$ (see Discussion). In the RR spectra of the native and dithionite-reduced forms, additional bands were detected at 1354 ± 1 ($\nu_4$), 1576 ± 1 ($\nu_2$), 340 ± 1 ($\nu_8$), and 1471 ± 1 $cm^{-1}$ ($\nu_3$) (Figure 6A−C and spectra not shown). The observation of RR contributions of reduced heme $c_i$ in the spectra of native cyt $b_6f$ (Figure 6B, spectrum b) suggests an autoreduction and/or a photoreduction under laser irradiation, a phenomenon very similar to that observed for oxidized cyt *f* (*13*).

RR contributions of the peripheral methyl and propionate heme groups have been determined in the mid- and low-frequency regions of the spectra of heme proteins (*30*, *31*). The 900−1300 $cm^{-1}$ region of the RR spectrum of *Chlamydomonas* cyt $b_6f$ excited at 441.6 nm, with the aim of enhancing *b* heme contributions, contains very intense carotenoid bands that hide the RR signals of the hemes (ref *13* and this work). Shifting the laser excitation to 413.1 nm allows one to detect more specifically heme modes in this region. However, the RR contribution of cyt *f* becomes

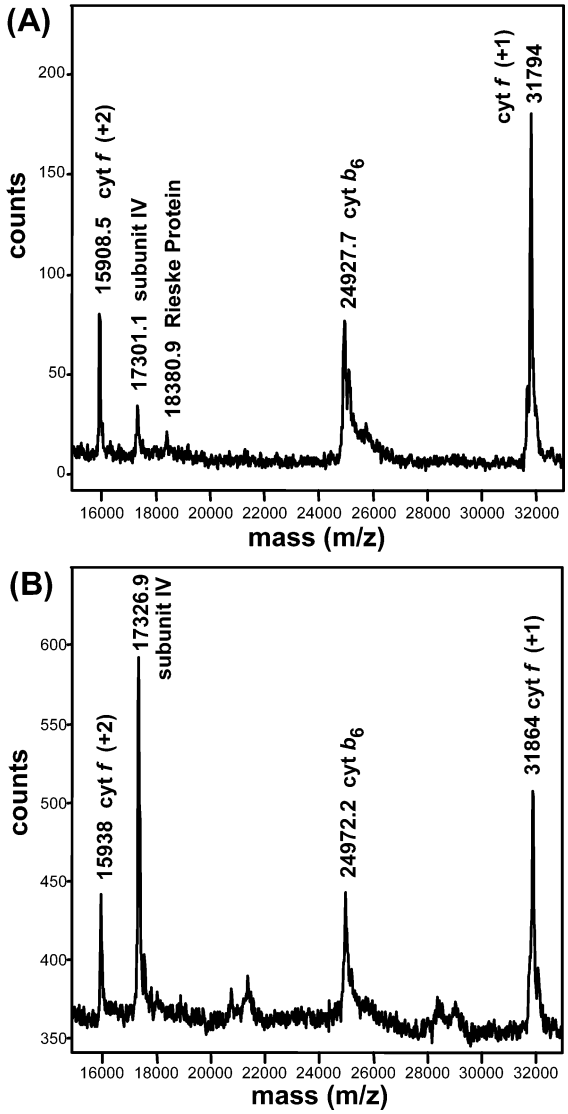


FIGURE 4: Mass spectrum of isolated $b_6f$ complexes of *Chlamydomonas*. (A) Complex with Rieske protein (purification with 20 mM HG and lipids). (B) Complex deficient in Rieske protein (purification with 30 mM HG without lipids).

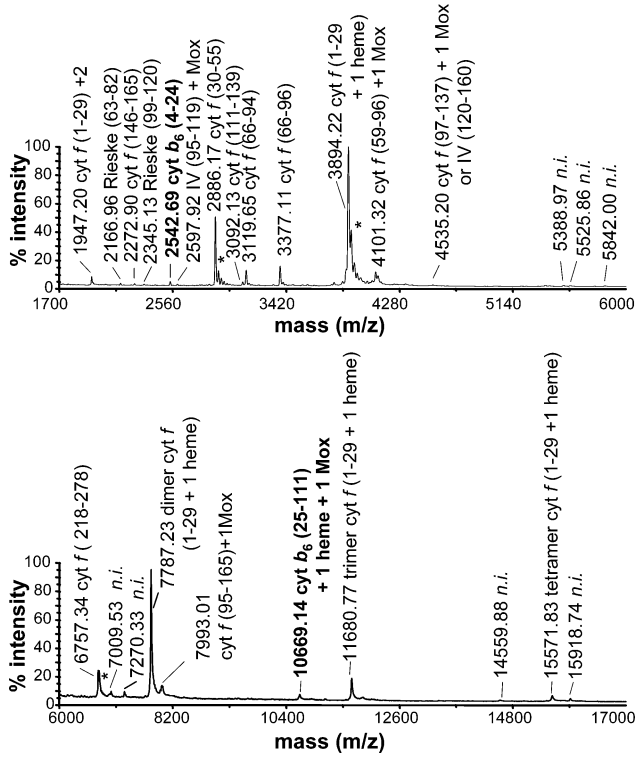


FIGURE 5: MALDI-TOF mass spectrum of monomeric $b_6f$ complexes of *Chlamydomonas* digested with Lys-C and analyzed with sinaptinic acid as a matrix in the positive and linear mode.

significant with this excitation. To overcome this problem, we recorded spectra from both the native complex, which displays reduced cyt *f* and oxidized cyt $b_6$ (Figure 7, spectrum a), and the dithionite-reduced complex containing fully reduced cyt *f* and cyt $b_6$ (Figure 7, spectrum b). The carotenoid bands are denoted on spectrum a. Since these bands should not be modified by the redox state of cyt $b_6f$ complexes (ref *13* and this work), the difference spectrum (dithionite-reduced minus native) mainly represents contributions of the reduced $b_6$ hemes (Figure 7, spectrum c). Bands observed at 999, 1082, 1170, 1213, and 1225 $cm^{-1}$ are in close correspondence with bands observed in the spectra of dithionite-reduced cyt $bc_1$ from *Rhodospirillum rubrum* (*11*). These are found at 1001 [$\nu(C_b$-vinyl)], 1081, 1172 ($\nu_{30}$), 1216 ($\nu_{42}$), and 1226 $cm^{-1}$ ($\nu_{43}$), respectively. Nevertheless, we detected several bands that show significant shifts to lower frequencies. A doublet is now observed at 1114 and 1129 $cm^{-1}$ in the cyt $b_6f$ spectrum when it was found at 1120 and 1133 $cm^{-1}$ in the cyt $bc_1$ spectrum. These bands assigned to $\nu_5$ and $\nu_{14}$ correspond to symmetric stretching modes of the $C_b$-methyl bonds [$\nu_s(C_b-CH_3)$]. A band observed at 963 $cm^{-1}$ in the spectrum of cyt $b_6f$ was found at 970 $cm^{-1}$ in cyt $bc_1$, where it was attributed to an elongation mode of the propionate (Pr) heme groups [$\nu(C_b-Pr)$]. Also, the $\nu_{45}$ mode [$\nu_{as}(C_b-CH_3)$] is seen at a lower frequency in the cyt $b_6f$ spectrum (990 $cm^{-1}$ for $b_6f$ vs 994 $cm^{-1}$ for $bc_1$). Opposite shifts are also observed, with a band at 1243 $cm^{-1}$ for the cyt $b_6f$ complex [$\nu_{13}$, $\delta(C_m-H)$] when it was detected at 1230 $cm^{-1}$ in the spectrum of the cyt $bc_1$ complex. In the low-frequency regions (100−600 $cm^{-1}$), the RR spectrum of the cyt $b_6f$ complex shows three bands with modified frequencies relative to the spectrum of the cyt $bc_1$ complex, i.e., at 286, 312, and 382 $cm^{-1}$ (spectra not shown). These bands were assigned to a deformation of the $C_b$ atoms with their substituents, a pyrrole tilt, and a deformation of the $C_b$−propionate groupings, respectively [$\nu_9$, $\gamma_6$, and $\delta(C_b-Pr)$, respectively] (*30*, *31*). Therefore, in addition to a nearly constant number of RR bands detected in the spectra of the $bc_1-b_6f$ complexes, which indicates a conserved symmetry of the *b*-type hemes between the two types of complexes, all the differences seen in the mid- and low-frequency regions are indicative of a change in the structure and/or the environment of at least one of the four methyl groups (1-, 3-, 5-, and 8-heme substituents) and/or at least one of the two propionate groups (6- and 7-heme substituents) of a *b*-type heme. It is difficult to precisely delineate the origin of the observed frequency shifts, a major reason likely relying on a significant coupling of the peripheral heme modes (*30*, *31*). It is worth noting that we detected no significant contribution of heme $c_i$ in the midfrequency regions. This observation is not unexpected taking into account the weak intensities of its high-frequency $\nu_2-\nu_4$ and $\nu_8$ modes.

The vibrational modes of the 2,4-vinyls have been characterized previously (*31*). Comparing the spectra of cyt $bc_1$ from *R. rubrum* and of cyt $b_6f$ from *Chlamydomonas*,

Table 2: Peptides Observed in MALDI-TOF Analysis of the Lys-C-Digested Monomeric $b_6f$ Complex

| | measured mass (Da)[a] | subunit, residues, modifications[b] | calculated mass (Da) | $\Delta m$[c] |
|---|---|---|---|---|
| 1 | 1947.20 | biprotonated cyt *f* (1−29) + 1 heme | 1947.10 | 0.10 |
| 2 | 2166.96 | Rieske (63−82) | 2168.47 | 1.49 |
| 3 | 2272.90 | cyt *f* (146−165) | 2273.57 | 0.67 |
| 4 | 2345.13 | Rieske (99−120) | 2345.76 | 0.63 |
| 5 | 2542.69 | cyt $b_6$ (4−24) | 2542.82 | 0.87 |
| 6 | 2597.92 | IV (95−119) + 1 Mox | 2597.23 | 0.69 |
| 7 | 2839.07 | ni | | |
| 8 | 2886.17 | cyt *f* (30−55) | 2886.33 | 0.16 |
| 9 | 2908.55 | cyt *f* (30−55) + 1 Na | 2908.33 | 0.22 |
| 10 | 2930.58 | cyt *f* (30−55) + 2 Na | 2930.33 | 0.25 |
| 11 | 3092.13 | cyt *f* (111−139) | 3091.95 | 0.18 |
| 12 | 3119.65 | cyt *f* (66−94) | 3119.72 | 0.07 |
| 13 | 3141.01 | cyt *f* (66−94) + 1 Na | 3141.72 | 0.72 |
| 14 | 3377.22 | cyt *f* (66−96) | 3377.01 | 0.21 |
| 15 | 3894.25 | cyt *f* (1−29) + 1 heme | 3894.22 | 0.03 |
| 16 | 3915.48 | cyt *f* (1−29) + 1 heme + 1 Na | 3916.22 | 0.74 |
| 17 | 3938.70 | cyt *f* (1−29) + 1 heme + 2 Na | 3938.22 | 0.48 |
| 18 | 4101.32 | cyt *f* (59−96) + 1 Mox | 4103.85 | 2.53 |
| 19 | 4118.58 | ni | | |
| 20 | 4535.20 | cyt *f* (97−137) + 1 Mox, IV (120−160) | 4533.32 (*f*), 4536.48 (IV) | 1.88, 1.28 |
| 21 | 5001.60 | ni | | |
| 22 | 5018.31 | cyt *f* (95−139) | 5016.89 | 1.42 |
| 23 | 5388.97 | ni | | |
| 24 | 5419.89 | ni | | |
| 25 | 5525.86 | ni | | |
| 26 | 5578.55 | ni | | |
| 27 | 5842.00 | ni | | |
| 28 | 6757.34 | cyt *f* (218−278) | 6756.87 | 0.47 |
| 29 | 6778.30 | cyt *f* (218−278) + 1 Na | 6778.87 | 0.57 |
| 30 | 7009.53 | ni | | |
| 31 | 7270.33 | ni | | |
| 32 | 7787.23 | dimer [cyt *f* (1−29) + 1 heme] | 7788.44 | 1.21 |
| 33 | 7993.01 | cyt *f* (95−165) + 1 Mox | 7992.37 | 0.64 |
| 34 | 8009.16 | cyt *f* (199−273) | 8012.36 | 3.20 |
| 35 | 10669.14 | cyt $b_6$ (25−111) + 1 Mox + 1 heme | 10665.53 | 3.61 |
| 36 | 11680.77 | trimer [cyt *f* (1−29) + 1 heme] | 11682.66 | 1.89 |
| 37 | 14559.88 | ni | | |
| 38 | 15571.83 | tetramer [cyt *f* (1−29) + 1 heme] | 15576.88 | 5.05 |
| 39 | 15918.74 | ni | | |

[a] The indicated masses correspond to protonated average masses. [b] cyt *f* peptide with heme (entry 15), cyt $b_6$ peptides (entry 5), and cyt $b_6$ peptide with heme (entry 35). Nonidentified measured masses are indicated (ni). [c] The mass differences observed between calculated and measured masses ($\Delta m$) are in accordance with the mass accuracy in the linear mode (0.01−0.1%).

the RR bands assigned to $\nu$(C═C) and $\nu$($C_b$−vinyl) modes proved to be very similar in frequency as well as in relative intensity (spectra not shown).

The RR spectrum of the Soret-excited *c*-type hemes (406.7 nm excitation) exhibits intense stretching modes of the thioether bonds [$\nu$($C_b$−S)] in the 682−692 $cm^{-1}$ region (Figure 8A,B) (*30*, *32*, *33*). This is consistent with the spectrum of isolated ferrous cyt *f* that exhibits a single $\nu$-($C_b$−S) mode peaking at 686 $cm^{-1}$ (*33*). The RR spectrum of persulfate-oxidized cyt $b_6f$ displays a very broad band in the 660−720 $cm^{-1}$ region (Figure 8A, spectrum a). Part of the band should originate from ferrous cyt *f* since the $\nu_4$ region (1350−1380 $cm^{-1}$) indicates a partial photoreduction of oxidized cyt *f* even under oxidizing conditions (ref *13* and this work). Most of the bands observed in the RR spectra of the native or ascorbate-reduced cyt $b_6f$ complex, excited at 406.7 nm, originate from reduced cyt *f* (Figure 8A, spectrum b). Therefore, using the relative intensities of the

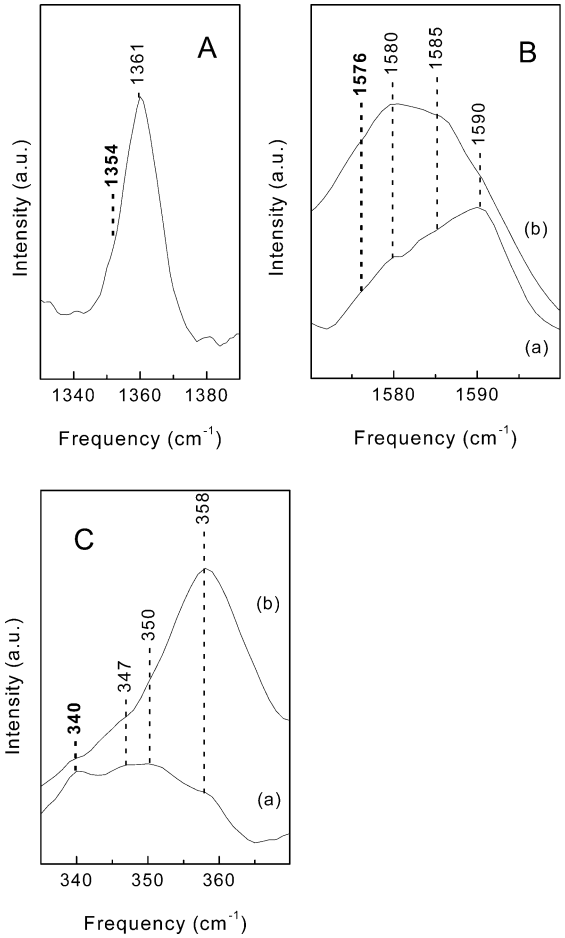


FIGURE 6: (A) $\nu_4$ region of the RR spectrum of dithionite-reduced cyt $b_6f$ excited at 441.6 nm. (B) $\nu_2$ regions of RR spectra of cyt $b_6f$ excited at 413.1 nm: (a) dithionite-reduced form and (b) native form. (C) $\nu_8$ regions of RR spectra of dithionite-reduced cyt $b_6f$ excited at 441.6 (a) and 413.1 nm (b).

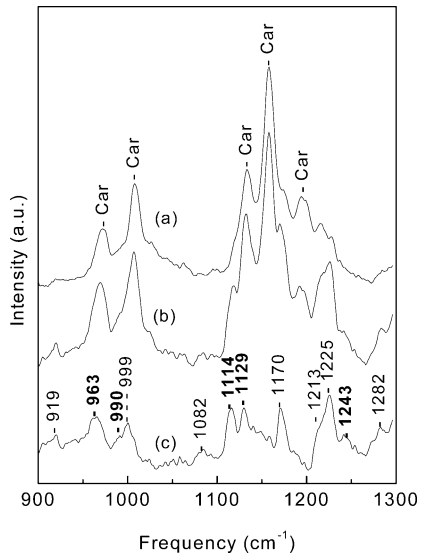


FIGURE 7: RR spectra (900−1300 $cm^{-1}$ regions) of the *Chlamydomonas* $b_6f$ complex excited at 413 nm: (a) native, (b) dithionite-reduced, and (c) difference spectrum (native minus dithionite-reduced). Spectra a and b were normalized using the intensity of the carotenoid bands (Car).

$\nu_4$ modes, it is possible to evaluate the contribution of photoreduced cyt *f* in the spectrum of oxidized cyt $b_6f$. Removal of this contribution in the 650−800 $cm^{-1}$ region

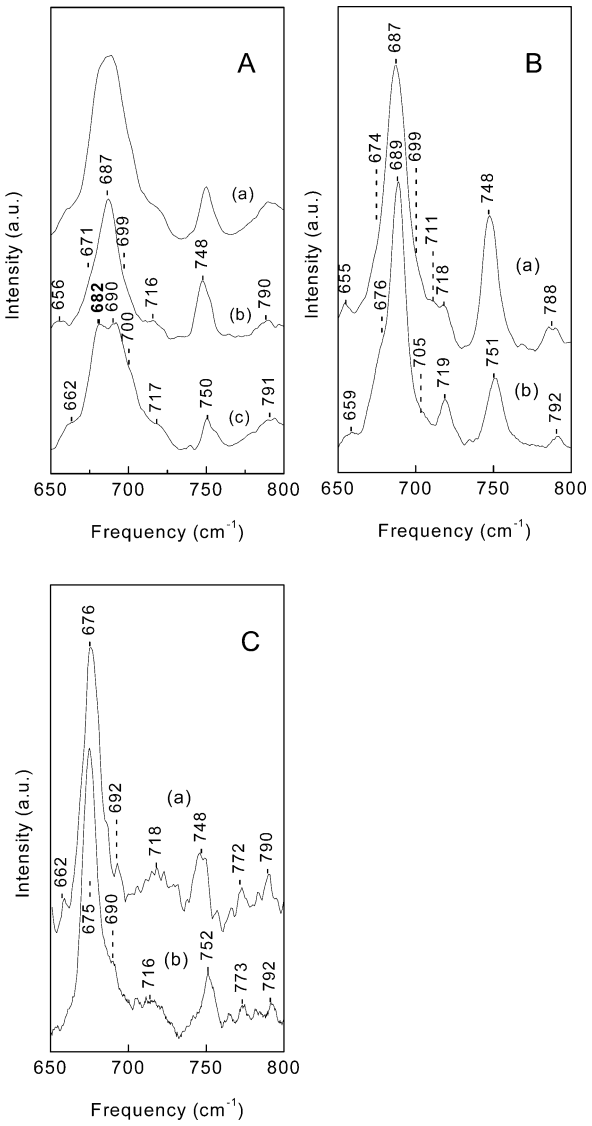


FIGURE 8: (A) RR spectra (650−800 $cm^{-1}$ regions) of the *Chlamydomonas* $b_6f$ complex excited at 406.7 nm: (a) persulfate-oxidized complex, (b) native complex, and (c) difference spectrum (spectrum a − 0.45 × spectrum b). (B) The 406.7 nm-excited RR spectra (650−800 $cm^{-1}$ regions) of the dithionite-reduced *Chlamydomonas* $b_6f$ complex (a) and of dithionite-reduced *R. rubrum* $bc_1$ (b). (C) The 441.6 nm-excited RR spectra (650−800 $cm^{-1}$ regions) of dithionite-reduced *Chlamydomonas* $b_6f$ complex (a) and of dithionite-reduced *R. rubrum* $bc_1$ (b).

produces spectrum c in Figure 8A. In the 670−710 $cm^{-1}$ region of this spectrum, we can now clearly identify three bands at 682, 690, and 700 $cm^{-1}$. To understand the origin of each of these bands, we investigated the 650−800 $cm^{-1}$ region of the RR spectrum from dithionite-reduced cyt $b_6f$, still excited at 406.7 nm (Figure 8B, spectrum a). As expected, this spectrum again contains major contributions from reduced cyt *f* (compare with spectrum b of Figure 8A). The general features are also very close to those of reduced cyt $bc_1$ from *R. rubrum* (Figure 8B, spectrum b). However, we observe a significant broadening toward the low-frequency side of the $\nu(C_b-S)$ mode of cyt *f* (687 $cm^{-1}$) when compared to the corresponding mode of cyt $c_1$ from cyt $bc_1$ (689 $cm^{-1}$) (Figure 8B). We take this broadening as an indication of the contribution of the $\nu(C_b-S)$ mode from cyt $c_i$ that is also responsible for the 682 $cm^{-1}$ band resolved in spectrum c of Figure 8A (see Discussion).

The 441.6 nm excitation enhances the RR contributions of the ferrous low-spin *b*-type hemes of $bc_1-b_6f$ complexes (*11*, *13*). Using this excitation, the spectra of reduced *Chlamydomonas* $b_6f$ and of reduced *R. rubrum* $bc_1$ are very similar (Figure 8C). The 650−700 $cm^{-1}$ regions of the $b_6f$ spectrum exhibit a $\nu_7$ band at 676 $cm^{-1}$, but no strong additional line at 680−690 $cm^{-1}$, which would be attributable to a thioether bridge between a *b*-type heme and apocyt $b_6$ (Figure 8C). Therefore, the RR data clearly show that neither $b_h$ nor $b_l$ is covalently linked to the apoprotein through a cysteine residue.

*Site-Directed Mutagenesis of the Conserved Cysteine Involved in a Thioether Bond.* Covalent binding of *c*-type hemes occurs through a thioether linkage to cysteine residues. A cysteine is conserved specifically in cyt $b_6$ and in the few cyt *b* molecules that strongly bind a heme (see Table 3). It corresponds to $Cys^{35}$ in *C. reinhardtii* that has indeed been identified as the ligand of heme $c_i$ in the 3D structure of the protein complex.

Substitution of $Cys^{35}$ with Val (C35V) in *Chlamydomonas* had a dramatic effect. The C35V mutant was unable to grow phototrophically. Biochemical analysis of its thylakoid membrane proteins showed that the C35V substitution prevented the accumulation of most of the $b_6f$ complex subunits (Figure 9A). Probing cyt $b_6$ in the C35V mutant with specific antibodies revealed (Figure 9A) the typical immunoreactive doublet band (*14*) that is observed in mutants that are unable to bind heme $b_h$, the *b* heme proximal to heme $c_i$, and in the nuclear *ccb* mutant strains (Figure 9B). These nuclear mutants are impaired in tight binding of heme to cyt $b_6$ (*14*).

## DISCUSSION

The unusual tight binding of a heme to cyt $b_6$, which is responsible for its peroxidase activity under denaturing conditions (*14*), has been confirmed by mass spectrometry, both in *C. reinhardtii* (this work) and in spinach and *M. laminosus* (*15*). This observation raised a number of questions concerning the nature and the role of this heme. The 3D structure of the cyt $b_6f$ complex recently determined at 3.1 Å resolution in *C. reinhardtii* first revealed an additional heme $c_i$, bound to $Cys^{35}$ and liganded via a water molecule or a hydroxide ion to a propionate from heme $b_h$, that should belong to the *c*′ group (*16*). This finding was confirmed upon refinement at 3.0 Å of the analysis of the structure of cyt $b_6f$ from *M. laminosus* (*17*). No characterization of heme $c_i$ has yet been provided, and the study presented here is a first contribution to the biochemical, spectroscopic, and biogenesis characterization of this atypical new heme.

*One Heme Covalently Bound to Cyt $b_6$.* The peroxidase activity associated with cyt $b_6$ proved to be SDS-resistant and acetone acid-resistant, which strongly suggested a covalent binding. An extra mass associated with cyt $b_6$ was found using MALDI-TOF, a technique that should dissociate noncovalently bound ligands from their apoproteins (*34*, *35*). In the few cases where noncovalent interactions with a protein were preserved by MALDI-TOF, there was always a mixture of bound and free forms. This was the case with ferredoxin-NADP reductase, where both the apoprotein and holoprotein still containing flavin were detected (*36*), with the monomeric and heptameric pore-forming complex of

Table 3: Alignment of Partial Sequences of Cyt $b_6$ and *b* Subunits

| Species[a] | helix A[b] | $b_l$ | helix B[c] | $b_h$ | N[d] |
|---|---|---|---|---|---|
| Cleaved and tight binding | | | | | |
| *C. reinhartii* $b_6$ | FY**C**IGGITFTCFLVQVATGFAMTFYY | ... | SI**H**RWSASMMVLMMVL**H**VF | | 14 |
| Spinach $b_6$ | FY**C**LGGITLTCFLVQVATGFAMTFYY | ... | SV**H**RWSASMMVLMMIL**H**VF | | 14 |
| *Synechocystis* $b_6$ | FY**C**LGGLTLTCFLIQFATGFAMTFYY | ... | SI**H**RWSASMMVLMMIL**H**VF | | 14 |
| *B. subtilis b* | VY**C**FGGLTFFVTVIQVLSGMFLTMYY | ... | GM**H**HWGASLVIVMMFL**H**TL | | 14 |
| Not cleaved and loose binding | | | | | |
| *C. limicola b* | WYYFGGLGLFFFVIQILTGLLLLQYY | ... | QI**H**AWSANLMIMMLFI**H**MF | | 14 |
| *R. sphaeroides b* | MWIWGVVLAFCLVLQIVTGIVLAMHY | ... | YL**H**ANGASLFFIAVYL**H**IF | | 13 |
| *S. cerevisiae b* | WWNMGSLLGLCLVIQIVTGIFMAMHY | ... | YL**H**ANGASFFFMVMFM**H**MA | | 13 |
| *B. taurus b* | WWNFGSLLGICLILQILTGLFLAMHY | ... | YM**H**ANGASMFFICLYM**H**VG | | 13 |

[a] Species presenting a split cyt $b_6$ or *b* and binding of heme to cyt $b_6$ or *b* are given in the top part, and those with no split cyt *b* and no tight binding of heme to cyt *b* are given in the bottom part. [b] In helix A, a cysteine residue conserved only in species presenting a tight binding of a heme is in bold and underlined. [c] In helix B, histidine residues serving as axial ligands to heme $b_l$ and $b_h$ are in bold. [d] The number of amino acids (*N*) between the two histidines residue ligands in helix D.

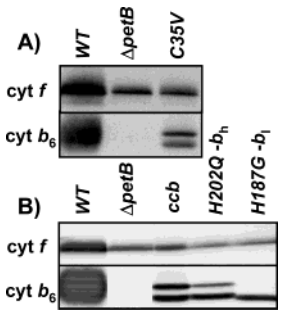


FIGURE 9: Immunodetection of mutants affecting cyt $b_6$. (A) Site-directed mutant of the chloroplast *petB* gene encoding cyt $b_6$ with a substitution of $Cys^{35}$ preventing thioether bonding of heme $c_i$ to Val (C35V mutant). (B) Nuclear mutant affecting specifically binding of heme to cyt $b_6$ (mutant *ccb*) and site-directed mutants of the chloroplast *petB* gene encoding cyt $b_6$ with a substitution of histidines involved as the axial ligand of heme $b_h$ preventing $b_h$ binding (H202Q mutant) or of heme $b_l$ preventing $b_l$ binding (H187G mutant). The wild-type (WT) and petB deletion strain (Δ*petB*) are shown as a reference.

*Aeromonas* toxin aerolysin (*37*), and with peptides associated or not associated with DNA (*38*). Here we identified by MALDI-TOF only one form of cyt $b_6$, the heme binding form, and no apoprotein, which indicates that the ligand is covalently bound to the protein. The smallest Lys-C proteolytic fragment detected by heme peroxidation of luminol is an internal fragment, $Tyr^{25}-Lys^{111}$, that we attributed to the first two transmembrane α-helices of cyt $b_6$. MALDI-TOF analysis of Lys-C fragments confirmed this attribution since the corresponding peptide was detected with an extra mass of 636 Da. This heme binding domain contains $Cys^{35}$, the covalent link of heme $c_i$ identified from the 3D structure. Thus, the biochemical data presented here are fully consistent with the structural data that demonstrate covalent binding of an extra heme to cyt $b_6$. It is of note that there are less than a handful of examples of a heme *c* attached by only one instead of two thioether bonds to their apoproteins, one in *Euglena gracilis* (*39*) and others in trypanosomatids (reviewed in ref *18*).

*Putative Additional Post-Translational Modifications.* Cyt $b_6$ from *Chlamydomonas* undergoes a covalent modification that increases its molecular mass by 801 ± 24 or 932 ± 24 Da depending on whether the initiation methionine is cleaved. This is still not known because cyt $b_6$ has a blocked N-terminus in *Chlamydomonas* (*22*), and we did not find any fragment containing the first three residues in our mass spectrometry spectra of cyt $b_6$ peptides. In addition, the first three N-terminal residues are not resolved at present in the *Chlamydomonas* structure (*16*).

When the heme contribution of 636 Da that corresponds to the extra mass observed with the $Cys^{35}$-containing Lys-C fragment is taken into account, cyt $b_6$ should still undergo some additional covalent modifications that raises its molecular mass by at least an additional 165 Da. Some chemical modifications may occur during sample preparation and analysis, like methionine oxidation, but the mass contribution of these changes is very limited. Phosphorylation of cyt $b_6$ in spinach has been previously reported (*40*). Electrospray ionization mass spectrometry detects an additional extra mass of 104.8 ± 1.2 Da in the heme-bound state of spinach cyt $b_6$ (*15*), for which one phosphate group of 80 Da could account. Phosphorylation occurs mainly at threonine and serine residues near the N-terminus of thylakoid membrane proteins (reviewed in ref *41*). A potential candidate for phosphorylation is a conserved serine at the N-terminus of cyt $b_6$. However, we have previously used phosphatase alkalin, under conditions that dephosphorylate photosystem II subunits and modify their band pattern (*42*). We did not observe any modification of the band pattern of cyt $b_6$ either in the wild-type strain which has a diffuse cyt $b_6$ band or in *ccb* or heme $b_h$ ligand mutants which have a cyt $b_6$ doublet band (data not shown).

*The b-Type Hemes Show No Covalent Binding to the Apocytochrome.* We compared the RR spectra of bacterial cyt $bc_1$ and monomeric *Chlamydomonas* cyt $b_6f$ to determine which new groups were specifically involved in protein−heme interactions in cyt $b_6$. We detected vinyl groups with intact double bonds for the *b*-type hemes of cyt $b_6$. From this result, any formation of a *c*-type thioether linkage between a cysteine residue and a vinyl group of the *b*-type hemes cannot be envisaged. We thus exclude the possibility that there would be a thioether linkage between heme $b_h$ and a cysteine residue in cyt $b_6$, as previously proposed on the basis of a cysteine mutation in *Bacillus subtilis* (*43*).

*Resonance Raman Vibrational Modes Identifying Heme $c_i$.* Monomerization of the cyt $b_6f$ complex with an increase in the concentration of the nonionic detergent HG above the critical micellar concentration released the chlorophyll molecule located between helices F and G of subunit IV in the cyt $b_6f$ structures (*16*, *17*). We then separated the monomer from the dimer and from free pigments. The RR spectra of *Chlamydomonas* cyt $b_6f$ were not significantly modified by monomerization: they exhibit features very similar to those of the dimeric form of spinach cyt $b_6f$ (*13*), in particular for the individual contributions of hemes $b_h$, $b_l$, and *f* to the skeletal $\nu_2$, $\nu_3$, and $\nu_8$ modes, respectively. However, the higher signal-to-noise ratio of the *Chlamydomonas* spectra allowed us to observe new RR contributions of a fourth heme component. The new bands observed at 1576 ($\nu_2$), 1471 ($\nu_3$), 1354 ($\nu_4$), and 340 cm$^{-1}$ ($\nu_8$) are tentatively assigned to heme $c_i$. These frequencies are characteristic of a ferrous *c*′-type heme under a five-coordinated high-spin state (*44*, *45*). The crystal structure identifies heme $c_i$ devoid of protein ligand in the axial position. On the face close to heme $b_h$, an oxygen atom of a water molecule or of a hydroxide ion is at a distance that is suitable for coordination of the iron atom. Ferroheme model compounds with one or two water, hydroxide, or alcohol ligands have been characterized (*46*−*49*). Besides a bis(aqua) complex that low-spin or intermediate-spin is (*48*), all other characterized ferrous compounds are high-spin. In particular, mono(hydroxide) and mono(aqua) complexes of ferroporphyrins exhibit spectral properties (absorption and RR) very similar to those of the corresponding five-coordinated high-spin mono(imidazole) complexes, modeling the axial coordination of ferrocyt *c*′ (*44*, *45*, *47*, *49*). Therefore, the set of frequencies observed for the $\nu_2-\nu_4$ and $\nu_8$ modes of heme $c_i$ is fully consistent with an axial coordination of water or hydroxide.

Water and hydroxide have a low affinity for ferrous porphyrins. However, a stabilizing environment can strengthen the binding of these weak oxygenated ligands by a factor ranging from 10 to $10^5$ (*50*). Absorption and RR investigations showed the formation of a five-coordinated high-spin mono(hydroxide) complex of Fe(II)-bound protoheme in an aqueous detergent solution. In this complex, the bound hydroxide group appears to be stabilized by the positively charged headgroups of the detergent micelle (*48*). As far as the water coordination is concerned, a mono(aqua) Fe(II) "picket-fence" porphyrin was characterized by RR spectroscopy as a five-coordinated high-spin complex (*47*). In such a complex, the coordinated water molecule is stabilized by H-bonding with one or two carbonyl groups of the porphyrin superstructure. A similar stabilizing condition seems to exist for the axially coordinated water or hydroxide of heme $c_i$. A carboxyl group of one of the propionates of heme $b_h$ is indeed at a distance and orientation necessary to form a strong H-bond with the axial ligand. Along this line, we observed perturbations of several peripheral heme modes. With respect to cyt $bc_1$, a change in the environment and/or conformation of one methyl and/or one propionate peripheral group(s) is observed for one *b*-type heme of the $b_6f$ complex. This effect is likely related to the close interaction between a propionate group of heme $b_h$ and the axial water or hydroxide ligand of heme $c_i$ (*16*).

Thioether linkage can be studied by RR through the $\nu(C_b-S)$ modes. In the 670−710 cm$^{-1}$ regions of RR spectra of oxidized cyt $b_6f$, there are three bands at 682, 690, and 700 cm$^{-1}$. The $\nu(C_b-S)$ frequency of reduced cyt *f* was assigned to 686−687 cm$^{-1}$ (*13*, *33*). Previous RR studies on various six-coordinated complexes of microperoxidase-8 showed that the frequency of its $\nu(C_b-S)$ mode is increased by 4−6 cm$^{-1}$ when the heme iron is oxidized (refs *51* and *52* and unpublished spectra). The 690 cm$^{-1}$ band is thus assigned to a $\nu(C_b-S)$ mode of oxidized cyt *f*. Its homologue in the spectra of oxidized cyt *c* was previously characterized at 693 cm$^{-1}$ (*30*). With reference to the RR spectra of oxidized cyt *c* (*30*), the 700 cm$^{-1}$ band is assigned to the $\nu_7$ mode of oxidized cyt *f*. The 682 cm$^{-1}$ band is a $\nu(C_b-S)$ mode originating from either oxidized cyt *f* or ferriheme $c_i$. Although reduced cyt *f* exhibits a single $\nu(C_b-S)$ mode at 686−687 cm$^{-1}$, the spectrum of oxidized cyt *f* could contain two $\nu(C_b-S)$ modes. However, the opposite occurs for cyt *c* with two identified $\nu(C_b-S)$ modes for the reduced state (682 and 692 cm$^{-1}$) and only one $\nu(C_b-S)$ mode for the oxidized state (693 cm$^{-1}$) (*30*). Alternatively, the additional 682 cm$^{-1}$ band could correspond to a thioether mode of heme $c_i$. The RR spectrum of reduced cyt $b_6f$, excited at 406.7 nm, also shows a broadening toward the low-frequency side of the 687 cm$^{-1}$ band that supports a heme $c_i$ assignment for the 682 cm$^{-1}$ band. We note that the RR spectrum of isolated cyt *f* in its reduced state does not exhibit such a band broadening (*33*) and *b*-type ferrous cytochromes do not have a band at this frequency.

*Is Heme $c_i$ either Photoreduced or Permanently Reduced?* Peroxidase activity resisting protein denaturation has been yet demonstrated only in *b* cytochromes that were split in two subunits. This is the case in cyt $b_6f$ complexes that exhibit cyt $b_6$ and subunit IV, being homologous to the N- and C-terminal moieties of cyt *b* from $bc_1$ complexes, respectively; it is also the case in *B. subtilis* where two proteins are found, cyt *b* and QcrC, a fusion of subunit IV and cyt *c* (Table 3). This might suggest a structural role of a tightly bound heme when the subunit is cleaved in two parts. The location of this additional covalent heme next to the plastoquinone binding site, "$Q_i$", blocking access to heme $b_h$, strongly suggests its participation in electron transfer from $b_h$ to plastoquinone. The distinction between a participation as a wire or through actual redox changes of its iron atom should be made on the basis of spectroscopic studies. Surprisingly, heme $c_i$ had not been observed spectroscopically in purified $b_6f$ complexes. This may be due in part to the fact that in the optical absorption spectra, the electronic bands expected for a *c*′-type heme in a five-coordinated high-spin state are broad and relatively weaker than those of the other cofactors of the cyt $b_6f$ complex. This heme should be

able to be detected by EPR, but the high-spin components in EPR spectra of purified $b_6f$ complexes (*51*) were (rather) attributed to heme denaturation and not to the presence of a $c'$-type heme. However, the EPR spectra would also be devoid of $c'$ heme contributions if heme $c_i$ were permanently reduced under the experimental conditions that have been employed.

Indeed, our high-frequency RR spectra identify heme $c_i$ as a ferrous heme. This ferrous heme may be either permanently reduced or sensitive to laser illumination. On one hand, a permanently reduced heme $c_i$ in the $b_6f$ complex would imply a very positive redox potential and, thus, the absence of a role in the mechanism of electron transfer in the $b_6f$ complex. On the other hand, oxidized heme proteins are prone to photoreduction by laser irradiations in the blue, violet, and near-UV regions. Among various factors, the nature of the axial ligand(s), the geometry of the axial coordination, the porphyrin distortion, and the surrounding media of heme play important roles in the photoreductive process (*52*, *53*). All these factors are also strongly involved in the determination of the redox potential of hemes. Ferric *c*-type cytochromes with largely positive redox potentials tend to be significantly sensitive to photoreduction. This is in particular the case for cyt *f* (*13*). No information about the redox potential of heme $c_i$ has been reported yet. Previous redox titration curves of the purified cyt $b_6f$ complex of *C. reinhardtii* did not reveal heme $c_i$ and indicated midpoint potentials of −158, −84, and 330 mV for heme $b_l$, heme $b_h$, and cytochrome *f*, respectively (*21*). The midpoint potential of cyt *G in vivo*, whose relation to heme $c_i$ remains to be established, was estimated to be 20 mV higher than that of heme $b_h$ (*18*, *19*). However, a weak field ligand, such as water or hydroxide, as well as the relatively polar environment of heme $c_i$ could facilitate photoreduction (*52*).

*Biosynthesis Pathway for Binding of Heme to Cyt $b_6$.* Substitution of the cysteine residue that covalently binds heme $c_i$ with a valine was a unique means of understanding the function of this new cofactor. Unfortunately, the C35V substitution in *Chlamydomonas* had a dramatic effect. The resulting mutant was unable to grow photoautotrophically and displayed a pleiotropic loss in all cyt $b_6f$ subunits. A similar loss in cyt *bc* complexes was observed when this conserved cysteine was replaced in *B. subtilis* (*43*).

From a biogenesis perspective, this strain that is unable to bind heme $c_i$ to cyt $b_6$ offered the opportunity to look at the folding and assembly of cyt $b_6$ in the absence of covalent heme binding. *In vivo*, *c* heme binding is assisted by several factors both in prokaryotes and in eukaryotes (reviewed in ref *54*). In *Chlamydomonas*, they are called the CCS factors and control the biosynthesis of cyt *f* and cyt $c_6$ (reviewed in ref *55*). There is no report that such factors would be mandatory for *b* heme binding. *In vitro*, hemin can bind without catalysis to synthetic peptides that mimic helices B and D of cyt *b* (*56*). Heme can also be reconstituted under denaturing conditions to a fusion protein of apocyt $b_6$ with maltose-binding protein in the absence of any other proteins (*57*). However, we had shown previously that conversion of apocyt $b_6$ to holocyt $b_6$ in *Chlamydomonas* is a specifically assisted process *in vivo* (*14*). We genetically identified at least four CCB nuclear factors involved in holocyt $b_6$ formation. Probing cyt $b_6$ with specific antibodies showed that the C35V mutant exhibited the double immunoreactive band (*14*) typical of the *ccb* nuclear mutants impaired in the binding of heme to cyt $b_6$. These results suggest that the CCB factors define the biogenesis pathway required for binding of heme $c_i$ to cyt $b_6$. Since this doublet band has also been observed in chloroplast *petB* mutants carrying substitutions of the histidines coordinating the $b_h$ heme (*14*), it is very likely that the covalent binding of heme $c_i$ and the noncovalent binding of heme $b_h$ are coordinated processes. Thus, the CCS pathway would be required for binding a hexacoordinated heme *c* with two thioether bonds on the typical CXXCH motif to cyt *f* and cyt $c_6$ on the lumenal side of the membrane, whereas the CCB pathway turns out to be specific for binding five-coordinated heme $c_i$ with one thioether bond on an atypical motif to cyt $b_6$ on the stromal side of the membrane.

## ACKNOWLEDGMENT

We gratefully acknowledge Y. Pierre for advice on $b_6f$ complex purification, J.-L. Popot and Y. Pierre for collaboration in cyt $b_6$ antipeptide production, and D. Picot and D. Stroebel for critical reading of the manuscript, stimulating discussions, and privileged communication of the cyt $b_6f$ complex structure.

## REFERENCES

1. Hope, A. B. (1993) The chloroplast cytochrome *bf* complex: a critical focus on function, *Biochim. Biophys. Acta 1143*, 1−22.
2. Cramer, W. A., Soriano, G. M., Ponomarev, M., Huang, D., Zhang, H., Martinez, S. E., and Smith, J. L. (1996) Some new structural aspects and old controversies concerning the cytochrome $b_6f$ complex of oxygenic photosynthesis, *Annu. Rev. Plant Physiol. Plant Mol. Biol. 47*, 477−508.
3. Hauska, G., Schütz, M., and Büttner, M. (1996) The cytochrome $b_6f$ complex: composition, structure and function, in *Advances in Photosynthesis, Volume 4, Oxygenic photosynthesis: the light reactions* (Ort, D. R., and Yocum, C. F., Eds.) pp 377−398, Kluwer Academic Publishers, Dordrecht, The Netherlands.
4. Berry, E. A., Guergova-Kuras, M., Huang, L.-S., and Crofts, A. R. (2000) Stucture and function of cytochrome *bc* complexes, *Annu. Rev. Biochem. 69*, 1005−1075.
5. Pierre, Y., Chabaud, E., Hervé, P., Zito, F., and Popot, J.-L. (2003) Site-directed photochemical coupling of cytochrome $b_6f$-associated chlorophyll, *Biochemistry 42*, 1031−1041.
6. Xia, D., Yu, C.-A., Kim, H., Xia, J.-Z., Kachurin, A. M., Zhang, L., Yu, L., and Deisenhofer, J. (1997) Crystal structure of the cytochrome $bc_1$ complex from bovine heart mitochondria, *Science 277*, 60−66.
7. Zhang, Z., Huang, L., Shulmeister, V. M., Chi, Y.-I., Kim, K. K., Hung, L.-W., Crofts, A. R., Berry, E. A., and Kim, S.-H. (1998) Electron transfer by domain movement in cytochrome $bc_1$, *Nature 392*, 677−684.
8. Iwata, S., Lee, J. W., Okada, K., Lee, J. K., Iwata, M., Rasmussen, B., Link, T., Ramaswamy, S., and Jap, B. K. (1998) Complete structure of the 11-subunit bovine mitochondrial cytochrome $bc_1$ complex, *Science 281*, 64−71.
9. Mosser, G., Breyton, C., Olofsson, A., Popot, J.-L., and Rigaud, J.-L. (1997) Projection map of cytochrome $b_6f$ complex at 8 Å resolution, *J. Biol. Chem. 272*, 20263−20268.
10. Breyton, C. (2000) The cytochrome $b_6f$ complex: structural studies and comparison with the $bc_1$ complex, *Biochim. Biophys. Acta 1459*, 467−474.
11. Le Moigne, C., Schoepp, B., Othman, S., Vermeglio, A., and Desbois, A. (1999) Distinct structures and environments for the three hemes of the cytochrome $bc_1$ complex from *Rhodospirillum rubrum*. A resonance Raman study using B-band excitations, *Biochemistry 38*, 1066−1076.
12. Schoepp, B., Chabaud, E., Breyton, C., Verméglio, A., and Popot, J.-L. (2000) On the spatial organization of hemes and chlorophyll in cytochrome $b_6f$. A linear and circular dichroism study, *J. Biol. Chem. 275*, 5275−5283.

13. Picaud, T., Le Moigne, C., Gomez de Gracia, A., and Desbois, A. (2001) Soret-excited Raman spectroscopy of the spinach cytochrome $b_6f$ complex. Structures of the *b*- and *c*-type hemes, chlorophyll *a*, and $\beta$-carotene, *Biochemistry 40*, 7309−7317.
14. Kuras, R., de Vitry, C., Choquet, Y., Girard-Bascou, J., Culler, D., Büschlen, S., Merchant, S., and Wollman, F.-A. (1997) Molecular genetic identification of a pathway for heme binding to cytochrome $b_6$, *J. Biol. Chem. 272*, 32427−32435.
15. Whitelegge, J. P., Zhang, H., Alguilera, R., Taylor, R. M., and Cramer, W. A. (2002) Full subunit coverage liquid chromatography electrospray ionization mass spectrometry ($LCMS^+$) of an oligomeric membrane protein: cytochrome $b_6f$ complex from spinach and the cyanobacterium *Mastigocladus laminosus*, *Mol. Cell. Proteomics 1.10*, 816−827.
16. Stroebel, D., Choquet, Y., Popot, J.-L., and Picot, D. (2003) An atypical haem in the cytochrome $b_6f$ complex, *Nature 426*, 413−418.
17. Kurisu, G., Zhang, H., Smith, J. L., and Cramer, W. A. (2003) Structure of the cytochrome $b_6f$ complex of oxygenic photosynthesis: tuning the cavity, *Science 302*, 1009−1014.
18. Lavergne, J. (1983) Membrane potential-dependent reduction of cytochrome $b_6$ in an algal mutant lacking photosystem I centers, *Biochim. Biophys. Acta 725*, 25−33.
19. Joliot, P., and Joliot, A. (1988) The low-potential electron-transfer chain in the cytochrome *bf* complex, *Biochim. Biophys. Acta 933*, 319−333.
20. Breyton, C., de Vitry, C., and Popot, J.-L. (1994) Membrane association of cytochrome $b_6f$ subunits. The Rieske iron−sulfur protein from *Chlamydomonas reinhardtii* is an extrinsic protein, *J. Biol. Chem. 269*, 7597−7602.
21. Pierre, Y., Breyton, C., Kramer, D., and Popot, J.-L. (1995) Purification and characterization of the cytochrome $b_6f$ complex from *Chlamydomonas reinhardtii*, *J. Biol. Chem. 270*, 29342−29349.
22. Breyton, C., Tribet, C., Olive, J., Dubacq, J.-P., and Popot, J.-L. (1997) Dimer to monomer conversion of the cytochrome $b_6f$ complex. Causes and consequences, *J. Biol. Chem. 272*, 21892−21900.
23. Thomas, P. E., Ryan, D., and Levin, W. (1976) An improved staining procedure for the detection of peroxidase activity of cytochrome P-450 on sodium dodecyl sulfate polyacrylamide gels, *Anal. Biochem. 75*, 168−176.
24. Kuras, R., and Wollman, F.-A. (1994) The assembly of cytochrome $b_6f$ complexes: an approach using genetic transformation of the green alga *Chlamydomonas reinhardtii*, *EMBO J. 13*, 1019−1027.
25. Kunkel, T. A. (1985) Rapid and efficient site-specific mutagenesis without phenotypic selection, *Proc. Natl. Acad. Sci. U.S.A. 82*, 488−492.
26. Goldschmidt-Clermont, M. (1991) Transgenic expression of aminoglycoside adenine transferase in the chloroplast: a selectable marker of site-directed transformation of *Chlamydomonas*, *Nucleic Acids Res. 19*, 4083−4089.
27. Boynton, J. E., Gillham, N. W., Harris, E. H., Hosler, J. P., Johnson, A. M., Jones, A. R., Randolph-Anderson, B. L., Robertson, D., Klein, T. M., and Shark, K. B. (1988) Chloroplast transformation in *Chlamydomonas* with high velocity microprojectiles, *Science 240*, 1534−1538.
28. Takahashi, Y., Rahire, M., Breyton, C., Popot, J.-L., Joliot, P., and Rochaix, J.-D. (1996) The chloroplast ycf7 (petL) open reading frame of *Chlamydomonas reinhardtii* encodes a small functionally important subunit of the cytochrome $b_6f$ complex, *EMBO J. 15*, 3498−3506.
29. Hu, S., Morris, I. K., Singh, J. P., Smith, K. M., and Spiro, T. G. (1993) Complete assignment of cytochrome *c* resonance Raman spectra via enzymic reconstitution with isotopically labeled hemes, *J. Am. Chem. Soc. 115*, 12446−12458.
30. Hu, S., Smith, K. M., and Spiro, T. G. (1996) Assignment of protoheme resonance Raman spectrum by heme labeling in myoglobin, *J. Am. Chem. Soc. 118*, 12638−12646.
31. Cartling, B. (1983) Intermediate and stable redox states of cytochrome *c* studied by low-temperature resonance Raman spectroscopy, *Biophys. J. 43*, 191−205.
32. Desbois, A. (1994) Resonance Raman spectroscopy of *c*-type cytochromes, *Biochimie 76*, 693−707.
33. Bordini, E., and Hamdan, M. (1999) Investigation of some covalent and noncovalent complexes by matrix-assisted laser desorption/ionization time-of-flight and electrospray mass spectrometry, *Mass Spectrom. 13*, 1143−1151.
34. Woods, A. S., and Huestis, M. A. (2001) A study of peptide−peptide interaction by matrix-assisted laser desorption/ionization, *J. Am. Soc. Mass Spectrom. 12*, 88−96.
35. Decottignies, P., Le Maréchal, P., Jacquot, J.-P., Schmitter, J.-M., and Gadal, P. (1995) Primary structure and post-translational modification of ferredoxin-NADP reductase from *Chlamydomonas reinhardtii*, *Arch. Biochem. Biophys. 316*, 249−259.
36. Moniatte, M., van der Goot, F. G., Buckley, J. T., Pattus, F., and van Dorsselaer, A. (1996) Characterisation of the heptameric pore-forming complex of the *Aeromonas* toxin aerolysin using MALDI-TOF mass spectrometry, *FEBS Lett. 384*, 269−272.
37. Lin, S., Cotter, R. J., and Woods, A. S. (1998) Detection of non-covalent interaction of single and double stranded DNA with peptides by MALDI-TOF, *Proteins Suppl. 2*, 12−21.
38. Mukai, K., Yoshida, M., Toyosaki, H., Yao, Y., Wakabayashi, S., and Matsubara, H. (1989) An atypical heme-binding structure of cytochrome $c_1$ of *Euglena gracilis* mitochondrial complex III, *Eur. J. Biol. Chem. 178*, 649−656.
39. Priest, W. J., and Hajduk, S. L. (1992) Cytochrome *c* reductase purified from *Crithidia fasciculata* contains an atypical cytochrome $c_1$, *J. Biol. Chem. 267*, 20188−20195.
40. Gal, A., Herrmann, R. G., Lottspeich, F., and Ohad, I. (1992) Phosphorylation of cytochrome $b_6$ by the LHC II kinase associated with the cytochrome complex, *FEBS Lett. 298*, 33−35.
41. Hansson, M., and Vener, A. V. (2003) Identification of Three Previously Unknown in Vivo Protein Phosphorylation Sites in Thylakoid Membranes of *Arabidopsis thaliana*, *Mol. Cell. Proteomics 2*, 550−559.
42. de Vitry, C., Diner, B. A., and Popot, J.-L. (1991) Photosystem II particles from *Chlamydomonas reinhardtii*. Purification, molecular weight, small subunit composition, and protein phosphorylation, *J. Biol. Chem. 266*, 16614−16621.
43. Yu, J., and Le Brun, N. E. (1998) Photosystem II particles from *Chlamydomonas reinhardtii*. Purification, molecular weight, small subunit composition, and protein phosphorylation, *J. Biol. Chem. 273*, 8860−8866.
44. Othman, S., Le Lirzin, A., and Desbois, A. (1993) A heme *c*-peptide model system for the resonance Raman study of *c*-type cytochromes: characterization of the solvent-dependence of peptide-histidine-heme interactions, *Biochemistry 32*, 9781−9791.
45. Othman, S., Richaud, P., Verméglio, A., and Desbois, A. (1996) Evidence for a proximal histidine interaction in the structure of cytochromes *c* in solution: a resonance Raman study, *Biochemistry 35*, 9224−9234.
46. Keilin, J. (1949) On the properties and nature of dihydroxyl-haem, *Biochem. J. 45*, 448−455.
47. Leondiadis, L., Momenteau, M., and Desbois, A. (1992) Raman evidence for the formation of a monoaquo adduct of iron(II) tetrakis((N-*tert*-butylcarbamoyl)phenyl)porphyrin. A model for hemoproteins at low pH, *Inorg. Chem. 31*, 4691−4696.
48. Barkigia, K. M., Palacio, M., Sun, Y., Nogues, M., Renner, M. W., Varret, F., Battioni, P., Mansuy, D., and Fajer, J. (2002) Air-stable, electron-deficient Fe(II) catalytic porphyrins. Characterization and molecular structures of rare high spin Fe(II) hexacoordinated porphyrins, *Inorg. Chem. 41*, 5647−5649.
49. Gomez de Gracia, A., Bordes, L., and Desbois, A. (2004) *Inorg. Chem.* (submitted for publication).
50. Maillard, P., Schaeffer, C., Tétreau, C., Lavalette, D., Lhoste, J.-M., and Momenteau, M. (1989) Unusual co-ordination of water to iron(II) amino acid basket-handle porphyrins, *J. Chem. Soc., Perkin Trans. 2*, 1437−1442.
51. Othman, S., Le Lirzin, A., and Desbois, A. (1994) Resonance Raman investigation of imidazole and imidazolate complexes of microperoxidase: characterization of the bis(histidine) axial ligation in *c*-type cytochrome, *Biochemistry 33*, 15437−15488.
52. Othman, S., and Desbois, A. (1998) Resonance Raman investigation of lysine and *N*-acetylmethionine complexes of ferric and ferrous microperoxidase. Influence of the axial ligation on the heme *c* structure, *Eur. Biophys. J. 28*, 12−25.
53. Nitschke, W., and Hauska, G. (1987) On the nature of the $g = 6$ EPR signal in isolated cytochrome $b_6f$ complex from spinach chloroplasts, *Biochim. Biophys. Acta 892*, 314−319.
54. Gu, Y., Li, P., Sage, J. T., and Champion, P. M. (1993) Photoreduction of heme proteins: spectroscopic studies and cross-section measurements, *J. Am. Chem. Soc. 115*, 4993−5004.
55. Le Moigne, C., Picaud, T., Boussac, A., Loock, B., Momenteau, M., and Desbois, A. (2003) Absorption and resonance Raman

investigations of ligand rotation and nonplanar heme distortion in bis-base low-spin iron(II)-tetrakis(*o*-pivalamidophenyl)porphyrin complexes, *Inorg. Chem. 42*, 6081−6088.
56. Thony-Meyer, L. (2002) Cytochrome *c* maturation: a complex pathway for a simple task? *Biochem. Soc. Trans. 30*, 633−638.
57. Dreyfuss, B. W., Hamel, P. P., Nakamoto, S. S., and Merchant, S. (2003) Functional analysis of a divergent system II protein, Ccs1, involved in *c*-type cytochrome biogenesis, *J. Biol. Chem. 278*, 2604−2613.
58. Robertson, D. E., Farld, R. S., Moser, C. C., Urbauer, J. L., Malholland, S. E., Pidikiti, R., Lear, J. D., Wand, A. J., De Grado, W. F., and Dutton, P. L. (1994) Design and synthesis of multihaem proteins, *Nature 368*, 425−432.
59. Króliczewski, J., and Szczepaniak, A. (2002) *In vitro* reconstitution of the spinach chloroplast cytochrome $b_6$ protein from a fusion protein expressed in *Escherichia coli*, *Biochim. Biophys. Acta 1598*, 177−184.

BI036093P